Protected: 2014 Conference Proceedings

Session	Presentation	Documents
KEYNOTE	Waste to Energy in the United States: State of the Industry Ted Michaels, President of the Energy Recovery Council	
SESSION 1: R&D 1	Paper #8 A Modified Species-group Approach to Simplify the Description of Phase Behavior of CO2-NH3-H2O System Yin Xu, Xi Liu, Baosheng Jin; Southeast University, NanJing, Jiangsu, China	Download Paper
	Paper #9 Physicochemical Study of the Products of Combustion and Thermal Shock on Polymeric Materials Eduardo. F. Herrera,1 Carmen. J. Navarro,2 Martha A. Espinoza,1 Lorena Carrasco,1 Guillermo Gonzalez,1 Manuel Roman,1 Michel Montelongo,1 Elias Ramírez,1 Jorge I. Carrillo,1 Alfredo Campos,1 Ramón Gómez1; 1Centro de Investigación en Materiales Avanzados Calle Cervantes # 120, Complejo Industrial Chihuahua, Chih, Mexico, 2Junta Central de Aguas y Saneamiento (JCAS), Chihuahua, Mexico	Download Paper
	Paper #13 Combustion of Contaminated Livestock in a Pilot-Scale Air Curtain Burner Paul Lemieux,1 Joe Wood,1 Worth Calfee,1 Brent Hall2; 1U.S. Environmental Protection Agency, RTP, NC,	Download Paper

Physicochemical Study of the Products of Combustion and Thermal Shock on Polymeric Materials

Paper # (9)
Presented at the 33rd International Conference on Thermal Treatment Technologies & Hazardous Waste Combustors
October 13-15, 2014
Baltimore, MD

Author Name: Eduardo. F. Herrera[1], Carmen. J. Navarro[2], Martha A. Espinoza[1], Lorena Carrasco[1], Guillermo Gonzalez[1], Manuel Roman[1], Michel Montelongo[1], Elias Ramírez[1], Jorge I Carrillo[1], Alfredo Campos[1] and Ramón Gómez[1]; Centro de Investigación en Materiales Avanzados Calle Cervantes # 120, Complejo Industrial Chihuahua, Chih, Mexico, OP: 31109[1], Junta Central de Aguas y Saneamiento (JCAS), Chihuahua, Mexico[1]

ABSTRACT

Currently many industries use functionalized nanomaterials in order to obtain better mechanical, thermodynamic and quantum properties in the manufacture of parts, furniture, toys, etc. However, there still are many unanswered questions about potential environmental impacts.

The aim of the study is to analyze, by means of scanning with electron microscopy and transmission chemically and morphologically, the release particles of functionalized materials produced with polymeric nanocomposites to obtain more effective flame retardants, UV resistance and antimicrobial protection and thus, determine if the exposure to thermal shock or burning of the functional materials could release nanoparticles harmful to health. Finally, find if there is some statistic dependence between concentration and the morphology of the particles analyzed.

Six samples were subjected to heat shock at the Center for Research in Advanced Materials SC (CIMAV) and three samples were burnt by a cone calorimeter in the Southwest Research Institute (SwRI) of San Antonio. Particles collected in the process through a MOUDI-110 collector, were characterized by electron microscopes, by photomicrographs and elemental analysis. The results were interpreted using statistical analysis to establish a correlation between the physical and chemical properties, determining if the nanoparticles released are significant.

The relevant results were those in which the interest additives were released [ZnO, Ag or Mg $(OH)_2$]. In thermal shock we find release of Zn and Mg. In both cases the morphological analysis, shown that the lacunarity, fractal dimension and circularity are very similar in heat shock as combustion. However, the Feret's diameter for thermal shock doubles the size of the particles in the combustion test. Combustion particles in cone calorimeter test, interest additive was not released [Mg $(OH)_2$].

INTRODUCTION

The massive use of polymeric materials in our daily lives is driven by its remarkable combination of properties such as low weight and ease of processing. The development of flame retardant materials and understanding of the phenomena that occur during combustion often require close collaboration between various fields of scientific

knowledge. The keys to understanding the behavior of polymers and fire in the main fire control processes, is divided into four sections:

•The basics of fire behavior and laboratory testing of polymer combustion.

•The flame retardant properties.

•The most representative flame retardants and their modes of action.

•What synergic effects emerge of combinations of polymer and retardants of flame[1]?

The use of nanoparticles is currently being used to improve the quality of the materials. They have been increasingly used as an alternative to traditional retardant of flame (TRF) to improve strength and delay the flame of polymeric materials that have advantages over TRF in terms of production, amount of additive, smoke and production carbon monoxide and recycling[2].

Basfar (2002) reports that the flame retardancy of polymers can be improved by the incorporation of chemical retardants. Foremost, the addition of these elements may influence the mechanical, thermal and electrical properties. All these properties are influenced by the chemical nature of the material and its conditions of flammability[3].

Wood fiber reinforced plastic composite represents an emerging class of materials that combine the favorable performance and cost attributes to both wood and thermoplastics. In addition they are sustainable for the environment[4].

Pyrolysis is one of the best methods to recover material and energy from waste polymers, since only about 10% of the energy content of waste plastic is used to convert scrap hydrocarbon[5].

Detailed knowledge of the halogenated derivatives and their possible formation mechanism could help to find the proper way to remove these harmful substances from pyrolysis oil, or to prevent their formation during pyrolysis processes[6].

Calorimetry tests help us to obtain relevant information you need to know about the material we use, such as the quantity of energy released and how it is released. Ignition timing of the sample, the calorific value of the product (MJ/kg), the total heat release (MJ/m^2), the total heat release (MJ/m^2), total heat release versus time, smoke production (m^2) and the physical behavior of the product[7].

The combustion gases contain relevant material for study. Until recently the emitted particles were not considered of great importance. But scientific basis raised the need to characterize physical, chemical and biological, the effect of these particles on the environment. Currently, given its tiny size and composition represent largely a factor of toxicity[8].

The idea of doing all the work came from the European Union project known as "*New high-quality mined nanomaterials mass produced for plastic and wood-plastic nanocomposites*" (MINANO) (Project Number: 263946, Call part identifier: FP7-NMP-2010-EU-Mexico). The purpose of this research was to determine the damage that could be produced by the nanoparticles extracted for mining process, and that are functionalized to enhance the properties of the materials used in the industry.

Unfortunately, in the Third World and the developing countries, the waste produced by these types of materials does not have a sustainable destination as they are used in indiscriminate incineration, brick kilns, among others. The share of us in the MINANO project was to identify if there was release of nanoparticles in thermal and mechanic processes, and also report on the life cycle analysis involved[9-11].

EXPERIMENTAL METHODS/ MATERIALS/ PROJECT APPROACH

The methodology can be divided into five related processes: thermal shock tests, tests calorimetry, combustion gas sampling, morphological and elemental analysis and statistical analysis.

THERMAL SHOCK TESTS

Thermal shock chamber AES SM-2105D was used to establish the temperature range and number of cycles to be applied to the samples. It was finally decided to use a temperature range (-40 ° C/85 ° C) and cycles ranged from (5 and 100) of the time available to carry out the experiment –each cycle consisting of 30 minutes. The samples used were polypropylene (PP) as with polyvinyl chloride (PVC), more nanoparticle aggregates Ag 33% + PP, Ag 15% + PP, Mg (OH) 2 + PP, ZnO + PVC sawdust +, Ag + PVC + wood sawdust and a targed grid. The target grid was submitted to termal shock to discard some contaminant elements from the materials used.

Fig. 1 Thermal Shock Chamber Associated Environmental Systems AES SM-2105D, coupled with MOUDI.

Figure 1 shows the equipment used for producing a thermal shock in the samples. To capture the particulates, a cascade impactor NANO MOUDI rotation flag MSP 8 stages with aerodynamic diameters of cut, all in mycras (d50) 18, 10 (1), 5.6 (2) 3.2 (3) 1.8 was also used (4) 1.0 (5) 0.56 (6) 0.32 (7) and 0.1 (8) When removing microns camera samples we proceeded to remove the grids for analysis.

SAMPE PREPARATION:

Sample preparation was carried out in the laboratory 1 Research Center for Advanced Materials (CIMAV), in electron microscopy. Figure 2 shows the procedure based on the following subsections:

a) Several samples, obtained from different industrial dependences were immersed in methanol for 20 minutes to remove any organic contaminants or debris that could alter the results of the experiment[12].

b) The electron microscope grids were placed with the carbon membrane contacting the samples and a third of the length thereof. They were also covered with aluminum foil to avoid direct contact with the adhesive tape that completely surrounds the sample.

c) All samples were placed previously under a heat lamp for 20 min to remove contamination from organic compounds.

d) All samples were subjected to heat shock (-40 ° C to 85 ° C).

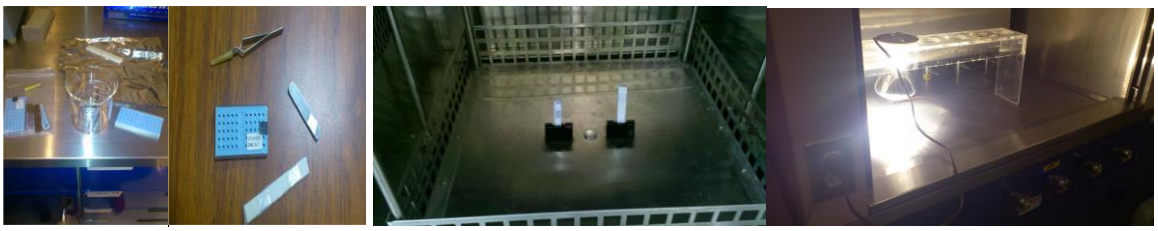

(a) (b) (c) (d)

Fig. 2 Process for the preparation of samples.

MATERIALS AND EQUIPMENT.

• Samples provided had (PP + 15% Ag, 33% Ag + PP, Mg (OH) 2 + PP, PVC + Ag + sawdust, ZnO + PVC + wood sawdust)
• Grids (Electron Microscopy Sciences) of copper with mesh 300 with carbon membrane for TEM.
• Grid Storage Boxes numbered to 50 pieces.
• Scotch Magic Tape
• Reynolds Foil
• Methanol
• Electron Microscopy Sciences brand Tweezers for handling TEM grids.
• Scissors.
• Chamber of heat shock (Associated Environmental Systems SM-2105D)
• Infrared lamp 120 V

TESTING CALORIMETRIC

The burning of the samples was conducted by the South West Research Institute (SwRI) in San Antonio Tx. These tests were run on a cone calorimeter brand Fire Testing Technology (Figure 3). The samples were made in the Administrative Services Peñoles based on ASTM E1354. The samples submitted to the combustion process were M1-871 (PVC + W), M1-872 (PVC + W + microns), M1-831 (PVC + W + nano).

Once the person responsible for running the tests calibrated equipment and prepared the sample, the gases were captured directly out of the hood through a hose to which a reduction was coupled at the end, were the gases entered. This hose was connected to MOUDI sucking the gases emitted by the ignition of the sample at 30 L/min. The impactor was kept in operation during the entire test. Generally it's only used in steps 7, 8 and 9.

After, the filters of the MOUDI and the grids were extracted for analysis.

Fig.3 Fire Testing Technology cone calorimeter in operation coupled to MOUDI-110

COMBUSTION GAS SAMPLING

To capture the particulates, a cascade impactor NANO-MOUDI rotation flag 8. MSP impactor operated at a flow rate of 30 ± 0.5 L / min for a sampling time of 10-15 minutes was also used.

Prior to the test, Teflon filters were placed in each stage of the equipment and as well as the microscope grids. In the first test the grids were placed in steps 1, 6 and 9, to observe the behavior of capture. The second and third tests were placed in steps 7, 8 and 9, since it was determined that the particles of interest were the smallest ones.

ELEMENTAL ANALYSIS

The elemental analysis was performed on electron microscopes (Figure 4). The particles intended for analysis were selected randomly, spectra were obtained by energy dispersive (EDS) X-ray. The magnifications were between X3, 000, x10, 000 and X100, 000 to the SEM and 120K-1M for TEM.

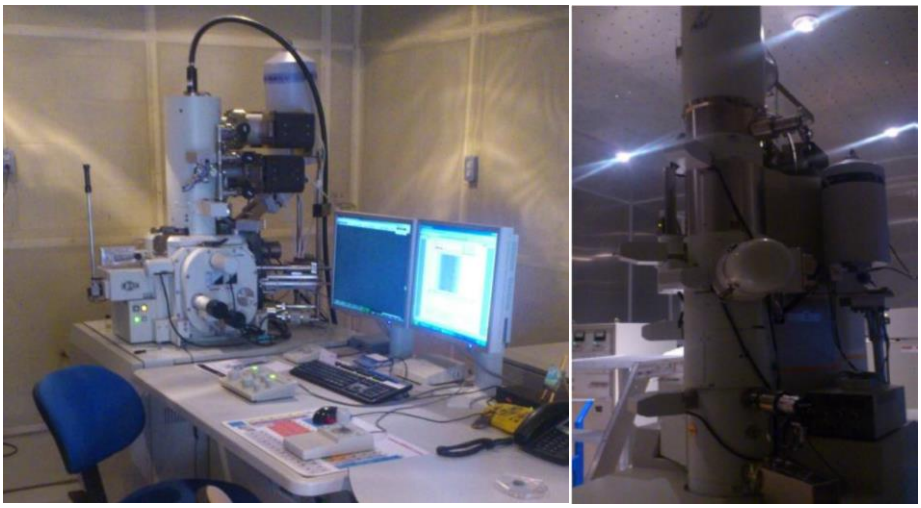

(a) (b)

Fig. 4 a) Scanning electron microscope SEM, b) TEM transmission electron microscope

MATERIALS AND EQUIPMENT

- Transmission electron microscope (TEM) JEOL 2200FS + CS
- Scanning electron microscope (SEM) JEOL JSM 7401F
- Grids (Electron Microscopy Sciences) copper with mesh 400 and carbon film on it, for the probing using TEM.
- Grid storage boxes numbered to 50 pieces

PREPARATION OF GRIDS SATURATED WITH MATERIAL RESULTING FROM COMBUSTION.

Figure 5 shows the method of preparing saturated grids based on the following subsections:
a) The grids in 1ml of methanol were placed.
b) Ultrasound for 5 minutes.
c) Once the particles are released in methanol, a drop of it was placed on the new grid using a capillary. The new grid is dried with infrared lamp for a few seconds until the liquid drop disappears.
d) Applied drops depended on the concentration of the solution to avoid saturating the grid[12].

Fig. 5 Grids saturation

MATERIALS AND EQUIPMENTS

• Ultrasound Branson 2510
• Methanol
• Electron Microscopy Sciences brand Tweezers for handling grids for TEM
• Infrared Lamp 120V
• Nitrile gloves.

MORPHOLOGICAL ANALYSIS

The Image J program was used to process images or micrographs. With this program some fractal parameters (see Table 1), such as area (Ap), perimeter (Pp), Feret diameter (Fmax), circularity, fractal dimension and lacunarity parameters were measured. Also, all the particles are subject to the EDS analysis. These analyzes were performed using the TEM. Figure 6 shows a graphic description of how the fractal parameters are measured.

IMAGE PROCESSING:

1-Al least 8-bit images must be used (Figure 7)
2-Set the scale with which it will work
3- Improve the brightness and contrast properly. (Figure 7 (a) and (b))
4- Apply the "threshold" that adjusts the lower and upper threshold of the active image.
5- Convert the image to binary image in order to work with the plugin FracLac built in ImageJ used to calculate fractal dimension and lacunarity.
6- Establish a selection of the particle to calculate area, perimeter, circularity and Feret diameter (Figure 8) Table 1.

Table 1. Fractal parameters[13]

Primary Measurements	Formula	Units
Perimeter	Pp	nm
Perimeter convex-hull	Pc	nm
Minimum radius of a circle from the center of mass	Rmin	nm
Maximum radius of a circle circumscribing the particle	Rmax	nm
Maximum Feret diameter	Fmax	nm
Minimum Feret diameter	Fmin	nm
Area	Ap	nm^2
Area convex-hull	Ac	nm^2
Fractal Dimension	D	

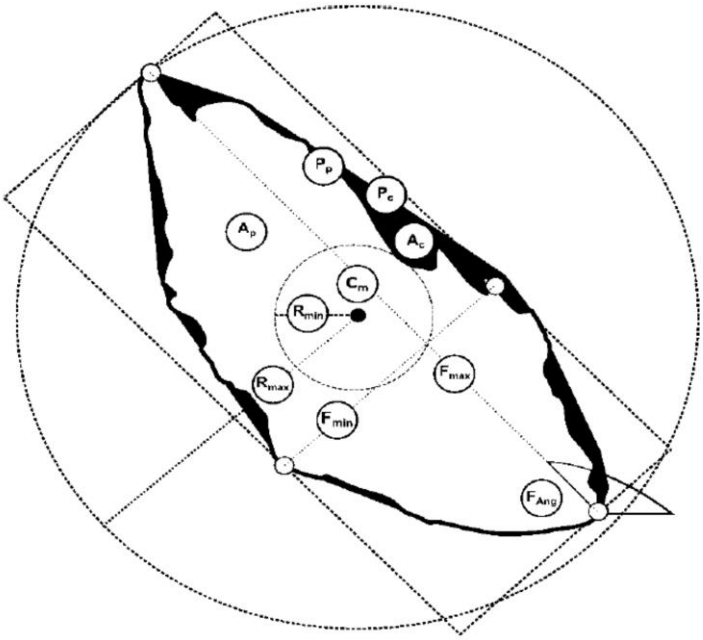

Fig. 6 Illustration with primary measures of a particle.

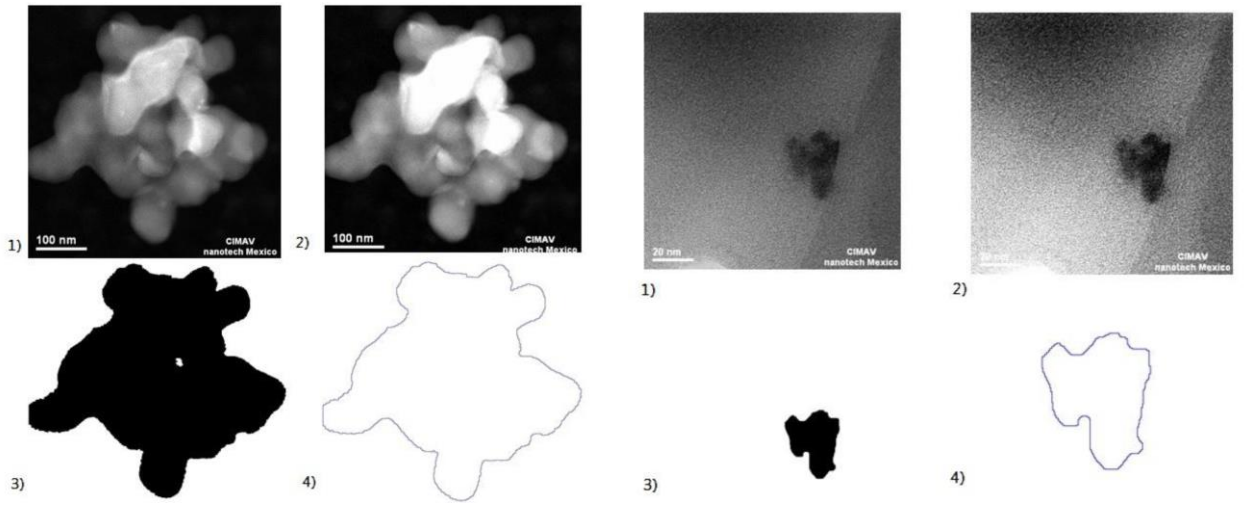

(a) (b)

Fig. 7 (a) Micrographs of combustion particles M1-872 material (PVC + W). (b) SEM micrographs of combustion of the material particles M1-871 (PVC + W)

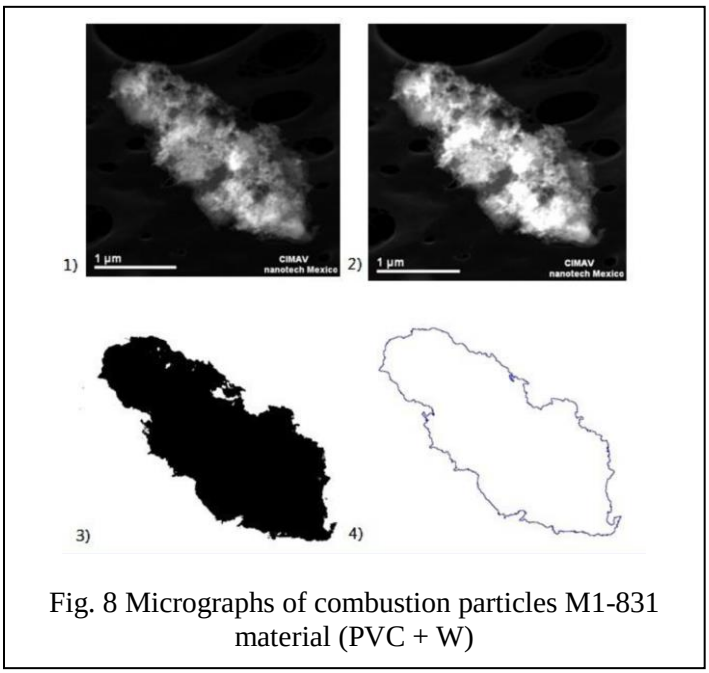

Fig. 8 Micrographs of combustion particles M1-831 material (PVC + W)

STATISTICAL ANALYSIS

An Excel database of the results of elemental analysis and particle morphology is created for better processing. The results were expressed on averages and graphics for better appreciation. However, complete tables are used for statistical analysis.

The techniques practiced for heat shock data were principal component analysis (PCA) for multivariate analysis. In addition, for linear regression the line graph adjusted and residual plots are used. For multivariate analysis is necessary to have a normal or linear data for processing. However, it was necessary to apply a Box-Cox due to the presence of bias and nonlinearity.

RESULTS AND DISCUSSION

THERMAL SHOCK.

CHEMICAL COMPOSITION: The basic analysis using electron microscope in the wood samples with PVC, PP, and additives Mg (OH) 2, ZnO and Ag, subjected to heat shock show that Mg and Zn particle release occurs, but not so with Ag particles, as shown in Figure 9. Nevertheless, some elements lacking interest S, Si, Cu, C, O. Ci, Al, among others, are produced by thermal shock. These elements could be justified for use in the PVC development process, are employed in the same experiment or are components of microscopy grids. Although the origin of some other elements is unknown, it can be caused by pollution in some stage of experimentation.

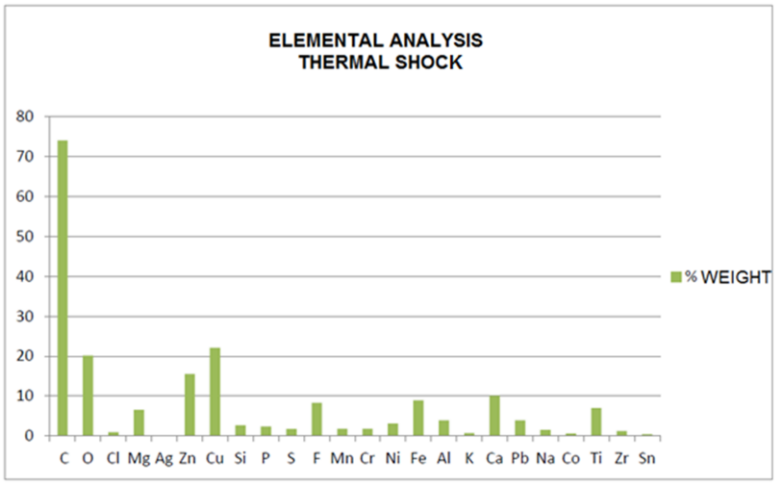

Fig. 9 Shown the average weight percent concentrations of the elements present in the particles released by heat shock.

MORPHOLOGY ANALYSIS

Table 2 shows the averages of the measured parameters of the particles giving us an idea of the size of the bodies. A database as this can be very useful in understanding the behavior and toxicity of the particles in the environment and in a living organism. The particles are $PM_{2.5}$ (fine particles) type that increases the risk of myocardium[14].

Table 2 shows the average measurements of particles subjected to heat shock.

	AREA (nm^2)	PERIMETER(nm)	DIAMETER OF FERET (nm)	CIRCULARITY	FRACTAL DIMENSION	LACUNARITY
Average	$1.6x10^6$	$5.2x10^3$	$1.5x10^3$	0.58	1.61	0.34

STATISTICAL ANALYSIS

The purpose of the multivariate analysis performed with Box-Cox data that was obtained from elementary analysis of heat shock, was to make the linear data and to obtain a better definition of correlation between them.

In Figure 10 it can be seen that the standardized remains curve detected by TEM is leptokurtic indicates that the data is not normal. Since the data should be normal to be used in the multivariate analysis, it was necessary to apply the Box-Cox transformation to correct biases, variances, and nonlinearity errors, as shown in the Figure 11.

The nanometric and micrometric samples with more quantity of elements detected were: Ag15% + PP, Ag + PVC, MDH + PP, ZnO + PVC.

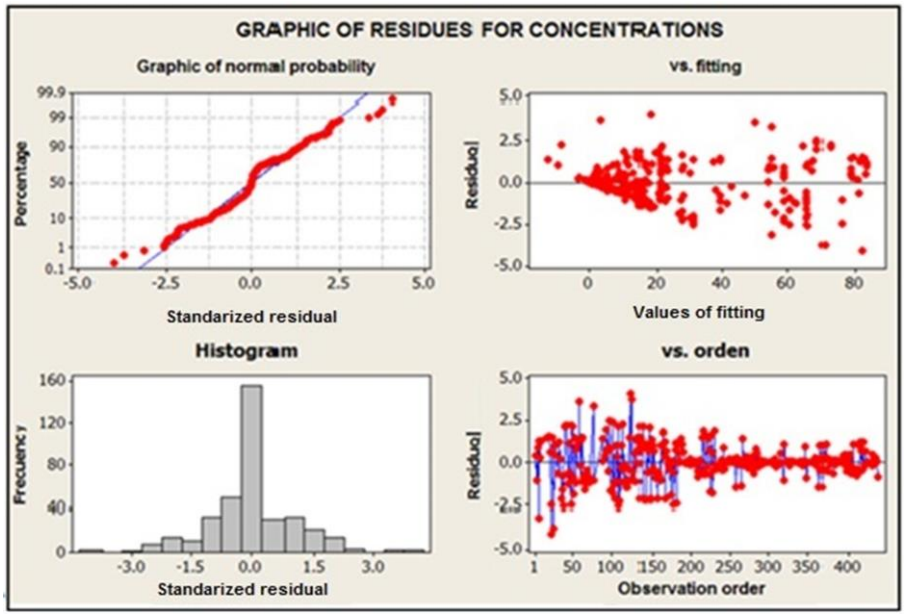

Fig. 10(a) Plot the residues of the concentration elements without Box-Cox

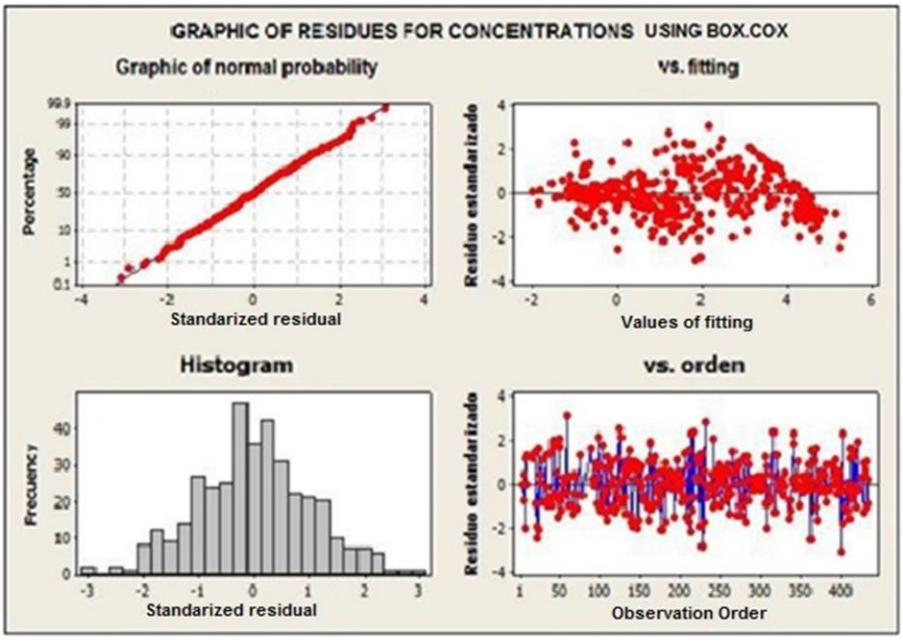

Fig. 11 Plot the residues of the concentration elements with Box-Cox.

In Table 3 are represented the samples and the most significant elements of their respective elemental and average Feret diameter analysis found. As can be seen the key elements are those that are found naturally in the materials such as C, O, Mg and Zn, because of the composition of the samples.

Table 3 . Variables in concentration percentages and average Feret diameter.

SAMPLE	Element Detected	Concentration Average (%W)	STDD CONS	VC (%) CONS	Dimension Average (nm)	STDD CONS (nm)	VC (%) ADIM	No. of Samples
Ag15%PP	C	88	23	26	3095	1838	59	13
	O	16	24	152	3065	1523	50	8
	Mg	0.42	0.08	19	3064	1632	53	2
	K	0.4	0.2	57	3064	1632	53	2
AgPVCDW	C	86	30	35	1397	1190	85	18
	O	17	23	137	2480	1881	76	4
MDHPP	C	66	26	40	1039	760	73	48
	O	22	15	68	1013	798	78	43
	Ca	11	10	84	1325	472	36	23
	Cl	0.5	0.4	73	1360	1469	108	6
	K	0.5	0.3	56	1424	245	17	5
	Fe	0.7	1	134	976	707	72	9
	P	0.3	0.1	33	1468	1321	90	6
Ag33%PP	C	85	25	30	1534	733	48	12
	O	12	9	75	1789	822	46	8
	Mg	0.9	0.5	58	1883	893	47	4
	K	0.44	0.02	5	1890	567	30	2
	Cr	0.7	0.5	71	2326	615	26	3
ZnOPVCWD	C	51	32	62	2198	1190	54	13
	O	23	19	83	2037	2796	137	10
	Zn	33	20	59	2589	3356	130	7

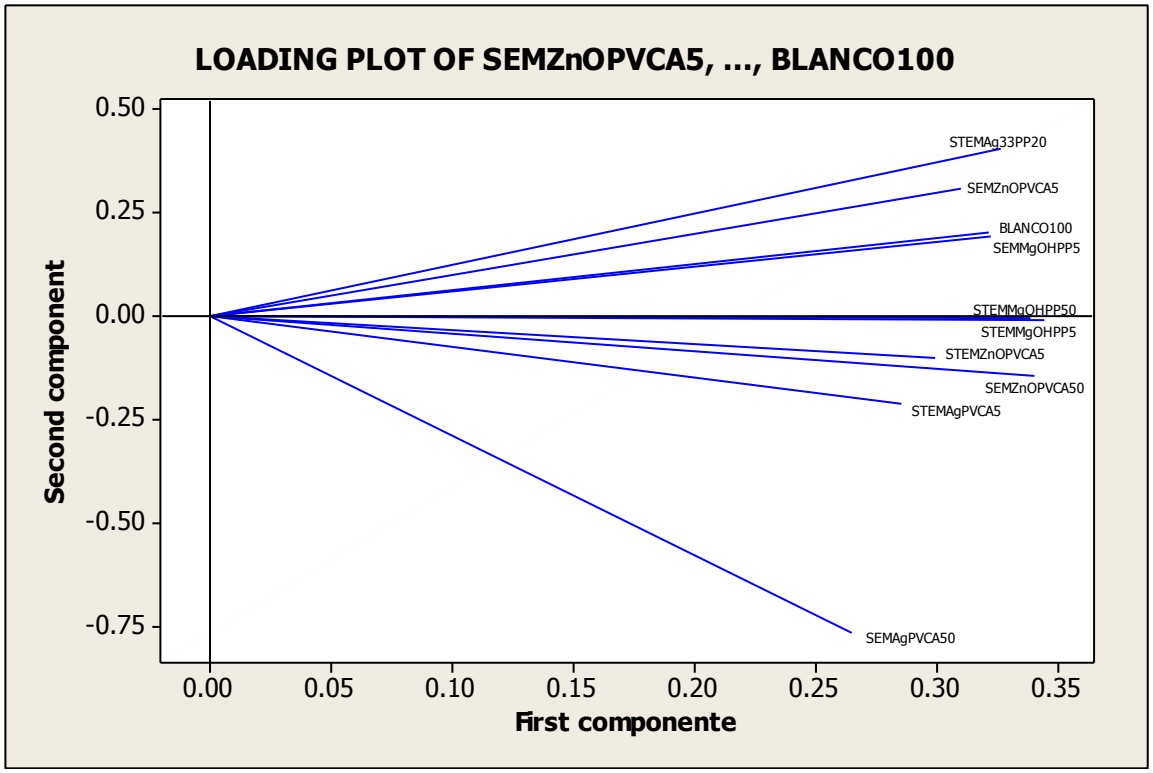

Fig. 12 Represents the Principal Components for the samples of heat shock.

Figure 12 shows the loading of the principal components calculated by mean of the elemental concentrations appearing in each of the particles observed in the electronic microscope, using the EDS analysis. The three first letters represent the type of analysis used in the microscope: The scanning transmission electron microscope (STEM) and scanning electron microscope (SEM). The last numbers after the name of the sample represent the numbers of cycles of thermal shock with the same values of temperature. Obviously, we can see that the behavior of the sample of silver and PVC, and fifty cycles of thermal shock (SEMAgPVCA50), is significantly different due to high concentrations of C and O, which marks a trend in the other elements that are issued in lower concentrations. However, I does not mean that is not releasing the compound of interest. We can also see that the smaller length vectors indicate significant differences due to the above, too.

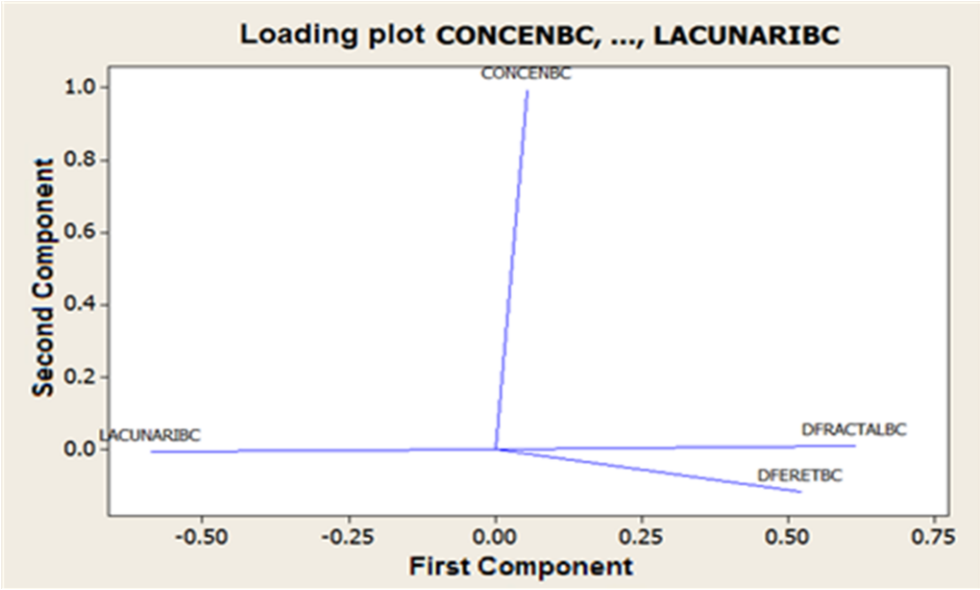

Fig. 13 Plot the principal components (and factors) of the fractal parameters treated with BOX-COX

Figure 13 shows the fractal parameters: lacunarity, Feret diameter and fractal dimension, compared to the elemental concentration in each of the particles, all of them processed through the Box-Cox transformation, hence the term of each denomination BC. Moreover, we can note in the same figure that the morphological characteristics have nothing to do with the elemental composition. This is because the vectors LACUNARIBC, DFRACTALBC and DEFERETBC are almost perpendicular to CONCENBC, while the morphological features (DFRACTALBC and DEFERETBC) are strongly correlated with each other, thus being inversely proportional to the lacunarity. Applying the VARIMAX rotation, the independence between elemental concentration and the morphological characteristics is more evident.

CONE CALORIMETER AND CHEMICAL COMPOSITION

Elemental analysis performed on an electron microscope in the cone calorimeter samples [M1-871 (PVC + W), M1-872 (PVC + W + microns), M1-831 (PVC + W + nm)] shows that no additive of interest is released [Mg (OH) 2]. Although Zn release occur as shown in the Figure 14. However, the samples do not contain Zn, but it is used in the manufacturing process of PVC. Here Ag was not added so it's normal that emissions appear in zeros.

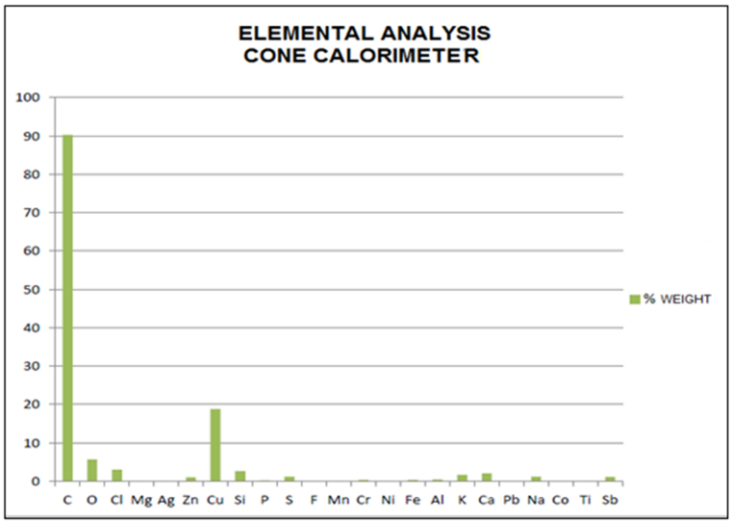

Fig. 14 Shown the average weight percent concentrations of the elements present in the particles released by combustion.

In none of the EDS analyzes performed at M1-871, M1-872 and M1-831 was found evidence of emissions of Mg from the combustion gases, despite having sufficient magnesium hydroxide in the form of nano and microparticles as flame retardants. However, the analysis of the ashes revealed large quantities of emissions (Figure 15).

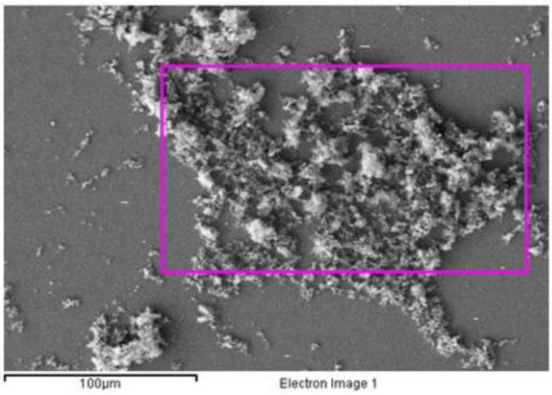

Fig. 15 SEM micrograph taken from the ashes of the samples M1-871, M1-872 and M1-831.

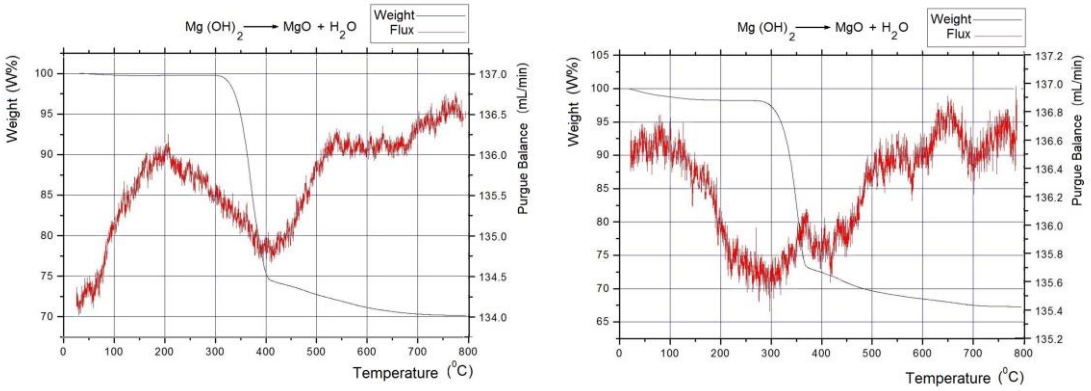

Fig. 16 Thermogravimetric analysis results for the additive Mg $(OH)_2$, a) Additive HQ2060 of microparticles; b) Additive NM-MX of nanoparticle.

In addition, thermogravimetric analysis to additive Mg $(OH)_2$ was carried out to confirm the presence of Mg in ashes. And, at the same time, observe their behavior as well as loss of mass with respect to time and temperature during the combustion process. Thus the experiment confirmed that the Mg remains in the ash, as discussed above. (Figure 16)

MORPHOLOGY ANALYSIS

In Table 4 we can observe the averages of the measured parameters of the particles, and also shows the size of the bodies found in stages MOUDI [18 (1), 0.56 (6) 0.32 (7) and 0.1 (8) microns]. The data may be useful to understand the behavior and toxicity of the particles in the environment or in a living organism. The particles are type PM1 (ultra-fine particles). This indicates that they could penetrate more deeply into the lung, the alveoli, and are strongly associated with severe health disorders[15].

Table 4 the average measurements of combustion particles are observed

	AREA (nm^2)	PERIMETER(nm)	DIAMETER OF FERET (nm)	CIRCULARITY	FRACTAL DIMENSION	LACUNARITY
Average	$2.3x10^5$	$2.8x10^3$	633.45	0.65	1.65	0.33

STATISTICAL ANALYSIS

To the results obtained from cone calorimeter were also applied a Box-Cox multivariate analysis. These analysis show absence of release of particles containing the additive of interest, here the $Mg(OH)_2$. In Table 5 (a) we can see certain elements are trendy and the most of them are those submitted to thermal shock, too. Similarly we can see the averages for the size and concentration. As for the size, the particles of combustion are smaller by 50% than the thermal shock due to the burning process and chemical reactions of the experiment.

Table 5) Values of concentration and Feret's diameter. b) Results of elemental analysis in the ash.

SAMPLE	Element Detected	Concentration Average (%W)	STDD CONS	VC (%) CONS.	Dimension Average (nm)	STDD DIM. (nm)	VC (%) DIM.	No. of Samples
M1-831	C	91	5	5	623	358	57	26
	O	6	3	50	623	358	57	26
	Cl	0.7	0.3	42	652	375	58	22
M1-871	C	85	13	15	698	808	116	32
	O	8	3	38	687	769	112	34
	Cl	8	9	113	776	784	101	39
	Si	6	9	150	766	864	113	31
M1-872	C	91	10	11	283	274	97	17
	O	2.0	0.4	20	287	284	99	16
	Si	1.0	0.8	80	690	180	26	13
	Cl	1	0.7	70	310	303	98	14
	Na	0.7	0.1	14	119	96	81	13

(a)

SAMPLE (only ash)	Element Detected	Concentration Average (%W)	STDD CONS	VC (%) CONS.	No. of Samples
M1-831	Mg	5	3	60	14
M1-871	Mg	21	11	52	14
M1-872	Mg	26	9	35	15

(b)

The elements that are found in high concentrations remain the C, O, Si, Cl and Cu, these being the ones that produce a very strong trend on the others. [Table 5 (a)].

For the Table 5 (b) is easy to see that all the Mg remained in the ashes of the analyzed material. Therefore, the additive satisfies with its functions as flame retardant because it remains in the ash after burned.

For the Feret's diameter and the fractal dimension, the most significant sample for particle size and morphology was the M1-831 and lacunarity was the M1-871. Similarly to thermal shock, the morphological data and linear trends are significantly equal in each component separately. This means that the behavior of particles released is equal in the concentration and morphology by separately. Nevertheless, willing to make an interaction between both analyzes is meaningless by the lack of correlation between them. (Figure 17)

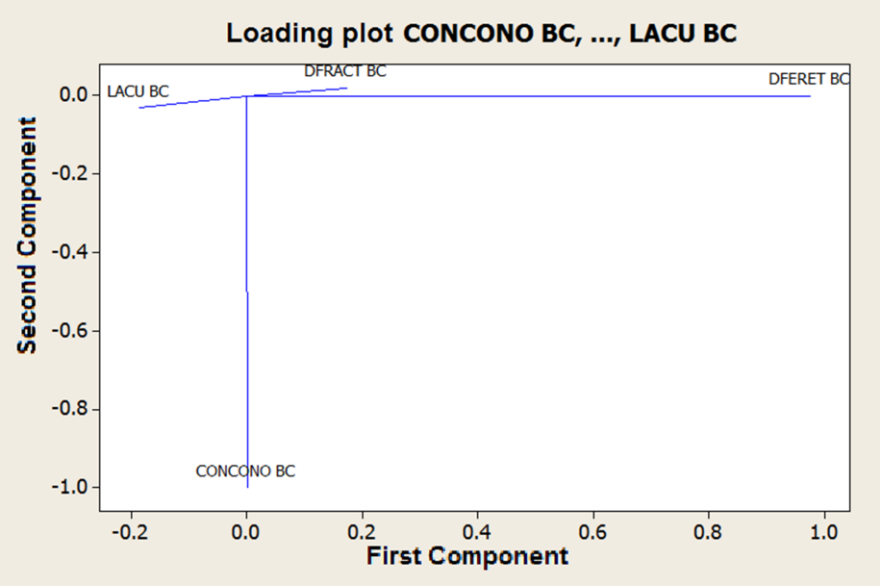

Fig. 17 Plot of Principal Factors rotated by VARIMAX

Finally, in the same Figure 17 we see that indeed the elemental concentration in the samples burned in the calorimeter cone (CONCONO BC) is not correlated with morphology (LACU BC, DFRAC BC and DFERET BC, all of them transformed by Box-Cox) . This is due to that the variance eigenvector of concentration is nearly 90 ° with the variance eigenvectors of the morphological parameters. We apply a VARIMAX rotation to align the axes. In addition, the lacunarity and the fractal dimension remain inversely proportional between them and the concentration is significantly different and any without correlation with the morphology.

SUMMARY

According to the results of statistical analysis, it is not possible to link the particulate morphology with the elemental composition of them (the null hypothesis is rejected and an alternative is accepted), because it does not exist correlation between these variables. There may be toxicity by the concentration or the fractal dimensions. However, in this case a synergism is discarded.

Statistical analysis shows that the thermal shock produces certain amount of releases of Mg. However, they are not representative with respect to the other elements; their behavior is the same, except with C, O, Si, and Ca.

Zn particles are released during the heat shock. However, according to the statistical analysis this is not representative because their behavior is very similar to the other elements.

The Ag release does not occur in any experiment, despite added to the heat-shock samples.

The morphology of the particles between the experiment of thermal shock and burn in the cone is very similar. This is based on the values of lacunarity, fractal dimension and circularity. However the Feret diameters in the thermal shock have double the size of the particles in the combustion. In this case particles of the order of $PM_{2.5}$ and $PM_{1.0}$ were obtained, which penetrate into the smallest ducts of the respiratory tract.

Statistical analysis of the cone calorimeter indicates that there is no release of the additive of interest, in this case the $Mg(OH)_2$. The function of the $Mg(OH)_2$ as flame retardant is so efficient that it is not released to the atmosphere, remains in the ash.

ACKNOWLEDGEMENTS

We gratefully acknowledge support by project MINANO, research cooperation among different institutes of the European Union and Latin America institutes (SAPSA, especially to Ph. D Ricardo Benavides), (OWENS), (CIQA), (UASLP) and (CIMAV).
A special acknowledgment to Professor Mika Paajanen VTT from Finland, chairman, for allowing us to participate in such an instructive exercise and also to Professor Stig Olsen DTU from Denmark for recommending the calculations of the life cycles analysis of the nanoparticles used in the entire project.

REFERENCES

1- Laoutid, B. A. (2008). New prospects in flame retardant polymer materials: From fundamentals to nanocomposites. *Material science and engineering* , 100-125.

2- Zhang, J., Delichatsios, M., & Bourbigot, S. (2009). Experimental and numerical study of the effects of nanoparticles on pyrolysis of a polyamide 6 (PA6) nanocomposite in the cone calorimeter. *Combustion and flame* , 2056-2062.

3- Basfar, A. (2002). Effect of various combinations of flame-retardant fillers on flammability of radiation cross-linked poly(vinyl chloride) (PVC). *Polymer Degradation and Stabilit* , 333-340.

4- Zhang, Z., Zhang, J., Lu, B.-X., Xiang, Z., Kang, C., & Kim, J. (2011). Effect of flame retardants on mechanical properties, flammability and foamability of PP/wood–fiber composites. *COMPOSITES* , 150-158.

5- Brebu, M., Bhaskar, T., Murai, K., Muto, A., Sakata, Y., & Uddin, A. (2004). The individual and cumulative effect of brominated flame retardant and polyvinylchloride (PVC) on thermal degradation of acrylonitrile–butadiene–styrene (ABS) copolymer. *CHEMOSPHERE* , 434-440.

6- Czégény, Z. (2012). Thermal decomposition of polymer mixtures of PVC, PET and ABS containing brominated flame retardant: Formation of chlorinated and brominated organic compounds. *Journal of Analytical and Applied Pyrolysis* , 69-77.

7- Chiltern International fire. (2012). *Chiltern International fire.* Recuperado el 22 de 09 de 2012, de http://www.chilternfire.co.uk/document/ti-1013-reaction-to-fire-cone-calorimetry-testin.pdf

8- López, G., & Estrada, A. (s.f.). *Biblioteca virtual de desarrollo sostenible y salud ambiental.* Recuperado el 22 de 05 de 2013, de http://www.bvsde.ops-oms.org/bvsaidis/caliaire/mexicona/R-0013.pdf

9-MINANO Project (2010). New high-quality mined nanomaterials mass produced for plastic and wood-plastic nanocomposites. No. 233946. Identifier: FP7-NMP-2010-EU-Mexico

10-**.** Paajanen, Mika; Benavides, R.; Olsen, S.; Rodriguez, O.; Aguilar, A.; Bellomo, L.o; Poppi, R.; Ruiz, F.; Zamudio, B.; Nieble, M.; Pasanen, Satu; Saarimäki, Eetta; Minkkinen, Hannu; Bocanegra, J.; Tena, C.; Deluna, G.; Martinez, J.-M.; Miseljic, M.; Morales, G.; Espinoza-Gonzalez, C.; Yanez, I.; Roman, M.; Gonzalez, G.; Herrera, E.; Orrantia, E.; Glossman-Mitnik, D.; Carfagnini, A.; Battelli, R. *New high-quality mined nanomaterials mass produced for plastic and wood-plastic nanocomposites*: General overview. VI International Conference on Surfaces, Materials and Vacuum, 23 - 27 September 2013, Mérida, Mexico

11- Miseljic, Mirko; Alvarado Diaz, Elsa Gabriela; Gonzalez Sanchez, Guillermo; Herrera Pereza, Eduardo Florencio; Olsen, Stig Irving. *Sustainability assessment of functionality enhanced polymers –engineered nanomaterials or conventional additives*. VI International Conference on Surfaces, Materials and Vacuum, 23 - 27 September 2013, Mérida, Mexico

12- David B. Williams and C. Barry Carter. Transmission Electron Microscopy. A Text Book for Materials Science, (2009). ISBN: 978-0-387-76500-6 (Print) 978-0-387-76501-3 (Online)

13- Trujillo, B. (2013). *Morfología y composición química de partículas del aerosol proveniente de fuentes fijas en la Cd. de Chihuahua, México.* Chihuahua (Tesis de Doctorado en Ciencia y Tecnología Ambiental, Centro de investigación de materiales avanzados).

14- Cocco, S., Polichetti, G., Spinali, A., & Trimarco, V. (2009). Effects of particulate matter (PM10, PM2.5 and PM1) on the cardiovascular system. *Toxicology* , 1-8.

15- Perrone, M.G., Guatieri, M., Consonni, V., Ferrero, L., Sangiorgi, G., Longhin, E., Ballabio, D., Bolzacchini, E., Camatini, M. (2013). Particle size, chemical composition, seasons of the year and urban, rural or remote site origins as determinants of biological effects of particulate matter on pulmonary cells. *Environmental pollution* , 215-227.

KEYWORDS

Mining, Nanoparticle, Life Cycle Analysis, Plastic, Wood-Plastic, Nanocompound, Flame Retardant, UV resistance, Antimicrobial, Fractal Dimension, Multivariant Analysis.